Experimental Astronomy manuscript No.
(will be inserted by the editor)

On the feasibility of studying the exospheres of Earth-like exoplanets by Lyman-α monitoring.

Detectability constraints for nearby M stars.

Ana I Gómez de Castro · Leire Beitia-Antero · Sabina Ustamujic

arXiv:1704.07443v1 [astro-ph.IM] 24 Apr 2017

Received: date / Accepted: date

Abstract Observations of the Earth's exosphere have unveiled an extended envelope of hydrogen reaching further than 10 Earth radii (R_E) composed of atoms orbiting around the Earth. This large envelope increases significantly the opacity of the Earth to Lyman-α (Lyα) photons coming from the Sun, to the point of making feasible to detect the Earth's transit signature from 1.35 pc with an 8 meter primary mirror space telescope, as we show. In this work, we evaluate the potential detectability of Earth analogues orbiting around nearby M-type stars by monitoring the Lyα flux variability. We show that, in spite of the interstellar, heliospheric and astrospheric absorption, transits in M-type stars would be detectable with a 4-8 m class telescope. A 2-m class telescope, such as the World Space Observatory would suffice to detect an Earth-like planet orbiting around Proxima Centauri. Such monitoring program would enable measuring the robustness of planetary atmospheres under heavy space weather conditions like those produced by M-type stars.

Keywords ultraviolet: planetary systems; planets and satellites: atmospheres

This work has been funded my the Ministry of Economy and Competitivity of Spain under grant numbers ESP2014-54243-R and ESP2015-68908-R

Ana I. Gómez de Castro
AEGORA Research Group, Universidad Complutense de Madrid, Plaza de Ciencias 3, 28040 Madrid, Spain
E-mail: aig@ucm.es

Leire Beitia-Antero
AEGORA Research Group, Universidad Complutense de Madrid, Plaza de Ciencias 3, 28040 Madrid, Spain

Sabina Ustamujic
AEGORA Research Group, Universidad Complutense de Madrid, Plaza de Ciencias 3, 28040 Madrid, Spain

1 Introduction

Atomic hydrogen is the dominant constituent of the upper terrestrial atmosphere. The primary source of atomic hydrogen is photodissociation by solar ultraviolet photons of molecular species (H_2O, CH_4, H_2) originated in the troposphere that are transported to higher altitudes (Brasseur & Solomon 1996, Dessler et al. 1994). Above 90 km, in the thermosphere, direct production of atomic hydrogen is balanced by upward diffusion with an estimated total escape flux of 10^8 cm^{-2} s^{-1}. This permanent loss of cold hydrogen atoms has a significant impact on long-term atmospheric evolution (Shizgal & Arkos, 1996).

Recent measurements have shown evidence of hot hydrogen atoms in the upper layers of the thermosphere. This population is generated by non-thermal processes and traces the coupling of the upper atmospheric layers to the plasmasphere, the magnetosphere and to space weather conditions in general (Qin & Waldrop, 2016). The interaction of hydrogen atoms with hot protons from the Solar wind and the energetic ions trapped in the ion belts leads to charge-exchange reactions and the production of energetic hydrogen atoms (1- 10^3 keV) that are key actors in the ion-neutral coupling between the atmosphere and magnetosphere. Hence, the precise determination of the atmospheric hydrogen distribution is vital for investigations of the chemistry, and the thermal and particle flow in the Earth atmosphere as well as its coupling with Solar activity.

The distribution of exospheric hydrogen is studied through the Lyman α (Lyα) transition, the most sensitive tracer to thin columns of neutral gas. Space probes detections show that the Lyα photons from the Sun are scattered by the hydrogen atoms in the Earth exosphere. Missions such as the Magnetopause-to-Aurora Global Exploration (IMAGE) satellite (Fuselier et al. 2000) or the Two Wide-angle Imaging Neutral-atom Spectrometers (TWINS) (McComas et al. 2009) have carried out these measurements while navigating within the exosphere. From these observations we know that there is an extended component of the exosphere, significantly stronger than predicted by the classical model (Chamberlain 1963).

The detection of exoplanets has opened the possibility of studying planetary exospheres in other planetary systems, submitted to diverse stellar radiation fields and space weather conditions. The transit of planetary exospheres in front of the stellar disk produces a net absorption that has been detected in the stellar Lyα profile. Since the seminal work by Vidal-Madjar et al. (2003) who detected the signature of HD209458b exosphere, Lyα absorption has also been detected from the hot Jupiter HD189733b (Lecavelier Des Etangs et al. 2010) and from the warm Neptune G436b (Ehrenreich et al. 2015). However, it has not been detected in the two super-Earths observed to date , namely 55 Cnc b (Ehrenreich 2012) and HD97658b (Bourrier et al. 2017). They have hypothesised that the lower extreme ultraviolet irradiation from these stars diminishes the hydrogen production rate in the thermosphere and hence, the

extent of the exosphere. However, it is possible that extended, Earth-like exospheres are not common or even undetectable with the current techniques.

Measuring the impact of dramatic enhancements of the solar activity on planetary exospheres had been unthinkable until the detection of Earth-like exoplanets. These are orbiting around extremely active stars, M dwarfs and Me stars, with strong magnetic fields and winds, thereby providing the ideal scenario to test Solar System-based planetary wind models under strong conditions. In this work, we evaluate the transmittance of the Earth to solar Lyα photons and compute theoretical Lyα light curves for the transit of an Earth-like planet orbiting around an M-dwarf star. We show that a 4-8 m class space telescope should be able to detect these variations. In Section 2 the transmittance of the Earth exosphere to Lyα photons is evaluated and in Section 3 the light curves are computed for Earth-like planets orbiting some sample stars. The potential of Lyα monitoring for the study of planetary exospheres is discussed in Section 4. A brief summary is provided in Section 5.

2 Transmittance of the Earth exosphere to Lyα photons

The GEO instrument (Mende et al. 2000) on board the IMAGE satellite found that the hydrogen density distribution is essentially cylindrically symmetric around the Sun-Earth line, exhibiting an enhancement in the antisolar direction, towards the geotail (Oestgaard et al. 2003, hereafter O2003). Along any given solar zenital angle, the density distribution is bimodal with a dominant central (or core) component and an extended component peaking at $\sim 8R_E$.

Later on, the TWINS mission obtained the 3D distribution of H I atoms between $3\mathrm{R}_E$ and $8\mathrm{R}_E$ and reported enhancements by a factor of 2-3 of the extended component with respect to O2003 (Zoennchen et al. 2011).

Therefore, the distribution of hydrogen in the Earth exosphere can be modelled for any given solar-zenital angle as,

$$n_H(r) = n_0 e^{-\frac{r}{r_0}} + \kappa n_1 e^{-\frac{r}{r_1}} \quad (1)$$

where r is the radial distance to the center of the Earth, (n_0, r_0) are the density and characteristic radius of the core component, dominated by the Earth photoevaporative flow, and (n_1, r_1) are the density and characteristic radius of the extended component. κ is a coefficient introduced to modify at will the relative strength of the extended component with respect to the core component. Minimum values of these coefficients are: $n_0 = 10^4$ cm^{-3}, $n_1 = 7 \times 10^{-3}$ cm^{-3}, $r_0 = 1.02R_E$, $r_1 = 8.2R_E$ and $\kappa = 1$ (O2003).

Using this distribution as a baseline, the column density of exospheric hydrogen (n_H) and the transmittance of the Earth's exosphere to stellar Lyα photons for a distant observer located on the plane of the ecliptic can be directly worked out. At a given projected distance, R, from the center of the Earth, the stellar Lyα photons propagate through a layer of thickness $2z_l = 2(r_e^2 - R^2)^{1/2}$, with r_e the radius of the exosphere taken to be 15 R_E

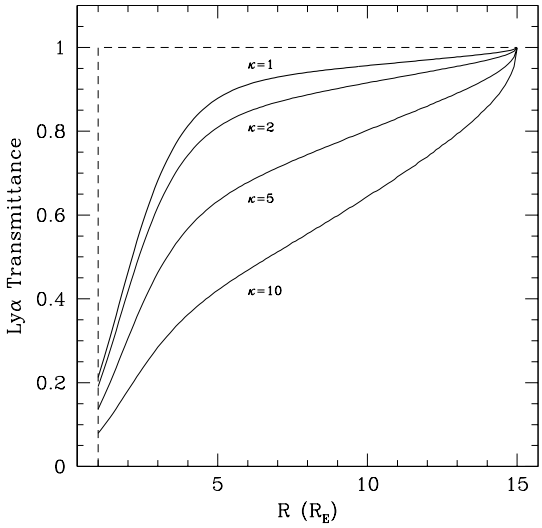

Fig. 1 Transmittance of the Earth's exosphere to Lyα photons in normal incidence from the Sun as a function of the radial distance to the center of the Earth (units: Earth radii (R_E)). κ indicates the relative strength of the extended component with respect to the baseline model obtained from IMAGE/GEO data (O2003). $\kappa = 1$ corresponds to the baseline model (bold). Measurements based on TWINS suggest $\kappa = 2 - 5$ (Zoenchen et al. 2010). The geometric cross-section of the solid Earth to solar Lyα photons is represented for guidance (dashed line).

for this calculation. The output radiation, $I(R)$, can be calculated from the standard radiation transfer equation,

$$\frac{dI}{I} = -\sigma n(r) dz, \tag{2}$$

being $z = \sqrt{r^2 - R^2}$ the depth of gas layer through which the Lyα radiation is being transferred and $\sigma = 5.9 \times 10^{-12} \times 1050^{-1/2}$ cm^2 (Bishop, 1999) the cross section of hydrogen to Lyα radiation; 1050 K is the reference temperature of the exospheric hydrogen (Bishop 1999, O2003).

This equation can be numerically integrated and for $dz << \sigma n(r)$ takes the form,

$$4\pi I(R) = \int_{-z_l}^{+z_l} I_0 \sigma n(r) dz \tag{3}$$

The transmittance of the Earth exosphere at a given projected distance is defined as,

$$T(R) = \frac{I(R)}{I_0} \tag{4}$$

and it is plotted in Fig. 1 for various possible $n(r)$ distributions; the reference curve is based on IMAGE/GEO results (O2003). We observe that at distances $> 3-4R_E$, the transmittance is very sensitive to the strength of the extended component. Additional transmittance curves enhancing the strength of the extended component by a factor of $\kappa = 2$, 5 and 10 with respect to O2003 are also represented; $\kappa = 2-5$ mimics well the results from TWINS (Zoenchen et al. 2011).

3 Calculation of the light curves for sample stars

Earth-like planets are being detected by the transit method: orbiting planets occult the stellar radiation when crossing the line of sight producing a measurable variation of the radiation that reaches the observer. The best suited stars for this purpose are M-dwarfs. They are the smallest and the most common class of stars in the Galaxy. GJ1132b (Berta-Thompson et al. 2016), Kepler-78b (Pepe et al. 2013), Kepler-93b (Dressing & Charbonneau 2015) or HD219134b (Motalebi et al. 2015) are some examples of positive detections of exoplanets around M stars. A candidate to Earth-like planet has been detected in Proxima Centauri, at 1.3 pc from the Sun (Anglada-Escudé, 2016).

We have computed transit light curves for two nearby M stars with well measured Lyα fluxes, namely AU Mic (M0 V) and Proxima Centauri (M5.5 V) (see Table 1 for the main parameters used in the calculation). Stellar Lyα fluxes for these stars have been evaluated by Wood et al. 2005; for our calculation, we have withdrawn the spectra from the Hubble archive and measured the *observed Lyα flux* to take into account the impact of interstellar, heliospheric and astrospheric Lyα absorption. In both cases, an Earth-like planet[1] is assumed to be orbiting in the habitable zone.

Table 1 Parameters used for the transit calculation.

Parameter	AU Mic	Prox Cen
Spectral Type$^{(a)}$	M0V	M5.5V
Radius ($R_\odot$)	$0.5^{(b)}$	$0.14^{(c)}$
Mass ($M_\odot$)	$0.6^{(d)}$	$0.12^{(e)}$
Semimajor axis of the orbit (a.u.)	0.3	0.032
$F_{Ly\alpha}(10^{-12}$erg cm^{-2}s$^{-1})^{(a)}$	10.3	4.21
logN_H (cm^{-2})$^{(a)}$	17.6	18.36
d (pc)$^{(a)}$	9.9	1.30

References: (a) Wood et al. 2005; (b) Rhee et al. 2007;
(c) Maldonado et al. 2015; (d) Chen et al. 2005;
(e) Benedict et al. 2016.

In addition, we have computed the light curve for the Earth-Sun system, as would be seen from a distance of 1.35 pc. This is the distance to α-Cen,

[1] An 'Earth-like' planet is assumed to have the same extended exosphere as the Earth?s.

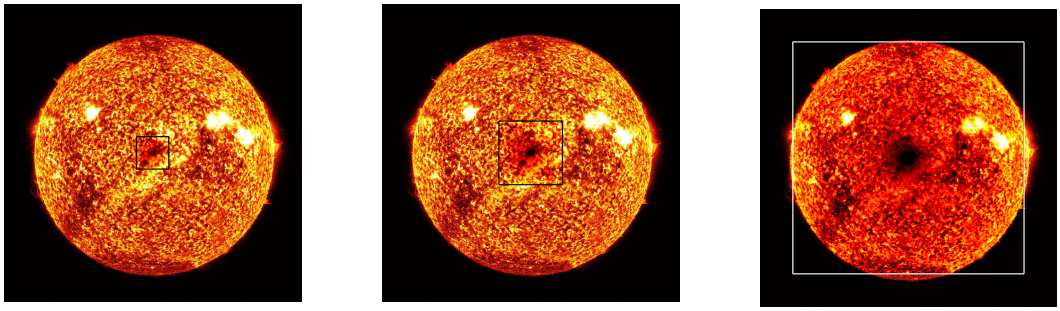

Fig. 2 Impact of the Lyα exospheric transmittance on the chromospheric emission; $\kappa = 2$ has been used for the transfer function. The transfer function has been applied to the Sun and to solar images, scaled to AU Mic and Prox Cen radii (from left to right). The central square has a size of $30R_E \times 30R_E$. Note that the geocoronal emission is not resolved in the figure.

the nearest analogue to the Sun. The Sun and α-Cen have similar Lyα fluxes and the Lyα absorption along the line of sight is well quantified (Wood et al. 2005). Note that the solar Lyα irradiance[2] at the Earth distance varies roughly between 3.5 and $6.5{\times}10^{11}$ photons cm^{-2} s^{-1} during the solar cycle (Rairden et al. 1986); we have adopted the highest value for the calculation.

The Lyα emissivity has been taken as constant over the stellar disk; the presence of dark spots and active regions has been neglected though the light curves could also be used to detect them. In all cases, the inclination is assumed to be 90^o (edge-on). The effect of the exospheric Lyα absorption is illustrated in Fig. 2; the Earth Lyα transmittance function has been multiplied by an image of the chromospheric solar radiation taken from the Solar Dynamics Observatory (SDO) archive to show the impact of the Earth's exosphere over the chromospheric emission, since Lyα comes from there. The absorption cross section is significantly enhanced with respect to the purely geometrical cross section produced by the Earth surface.

The theoretical light curves have been evaluated and projected into the observational space assuming a rather simple instrumental configuration and a 4 m primary mirror space telescope. The light path to the detector includes three reflections (primary, secondary and pick-off mirror) and an additional low dispersion grating to select the Lyα radiation. A grating is implemented instead of a filter because this is the most efficient configuration to filter the line radiation from a radiometric point of view (see, e.g. Gómez de Castro et al. 2014). The Lyα flux is assumed to be recorded with a photon counting CsI MCP detector with 20% quantum efficiency in the Lyα line. For the sake of the simulation, we have assumed a stable heliospheric background and have neglected the geocoronal emission, *i.e.* we hypotesise that the space telescope is high above the Earth corona, further than $4R_E$ (as the WSO-UV, see Sec. 4).

[2] https://lasp. colorado.edu/lisirg/lya

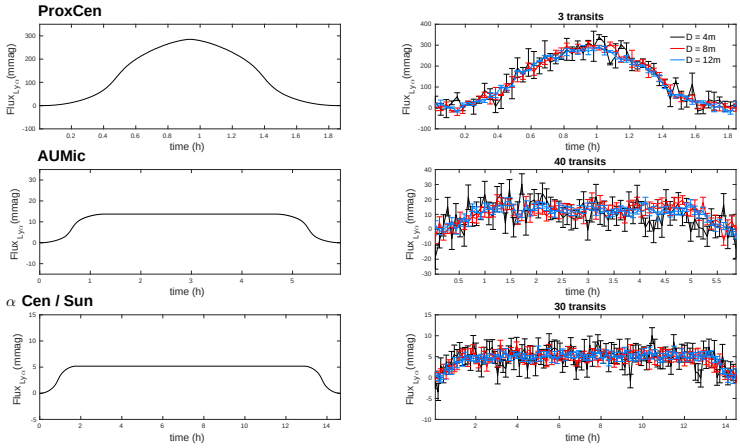

Fig. 3 Lyα light curves for the transit of an Earth crossing in front of the stellar disk. Stars are: Prox Cen (top), AU Mic (middle) and the Sun as seen from a distance of 1.35 pc (bottom). The theoretical model for the impact of the exosphere (assuming $\kappa = 2$) is represented in the left panel. The observed light curves, with a 4, 8 and 12 meters primary space telescope are plotted in the right panel.

The heliospheric background is taken to be 5.5×10^{-3} photons $cm^{-2}s^{-1}$ (Lallament et al. 1996); this background corresponds to the least favorable upwind orientation. In the model, the noise is dominated by the photon statistics.

Several planetary transits are co-added to increase the SNR (see right panel in Fig. 3). The different shapes of the light curves are due to differences in the stars' radii, transit duration and location of the habitable zone. According to these calculations , transits of an Earth-like planet orbiting around Prox Cen could be detected with a 4 m class space telescope. A larger primary (and an increasing number of passages) are required to detect a similar transit around AU Mic. The transit of the Earth in front of the Sun would be detectable from a distance of 1.35 pc using an 8 m class telescope (plus co-adding 30 observations of the transit).

4 Discussion: Potential exoplanetary studies using a Lyα monitor

Fig. 3 shows that extended, Earth-like exospheres produce a detectable absorption signature over stellar Lyα emission because of the strong opacity of the line and the large extent of the Earth exosphere. This signature is especially strong for small stars as M dwarfs but requires observation of transists with space telescopes orbiting high above the Earth geocorona. So far, Lyα observations of exoplanets exospheres only have been feasible with the Hubble Space Telescope (HST) that has a low Earth orbit. As a result, mid resolution, long-slit spectroscopy is required to remove the geocoronal emission and the sensitivity drops accordingly.

However, a telescope with capabilities similar to those of the Hubble Space Telescope, but in high Earth orbit like the WSO-UV (Shustov et al. 2015) will be able to run this kind of programs. WSO-UV is a 170 cm primary mirror space telescope that would be equipped with a solar-blind CsI MCP type detector optimised for the detection of Lyα photons. The far UV channel of the camera will be equipped with a prism for slitless spectroscopy providing a dispersion of 800 in the Lyα line to separate cleanly the line from nearby features. As shown in Fig. 4, an Earth orbiting in the habitable zone of Proxima Centauri will be detectable with WSO-UV.

Moreover, the distribution of hydrogen in the exosphere could be determined from the light curve for the most favorable case: Prox Cen. Note that the dip is more pronounced as κ increases. This sensitivity allows measuring the impact of stellar activity in the scale height of the hydrogen density distribution. In the Earth, the scale height increases with declining solar activity suggesting that the upper thermosphere is not a completely thermalized regime (Qin & Waldrop 2016) and that the energy input from collisions with magnetospheric and solar wind particles cannot be neglected. Extended exospheres have also been detected in Venus and Mars (Shizgal & Arkos, 1996) and it seems to be a common characteristic of terrestrial planets.

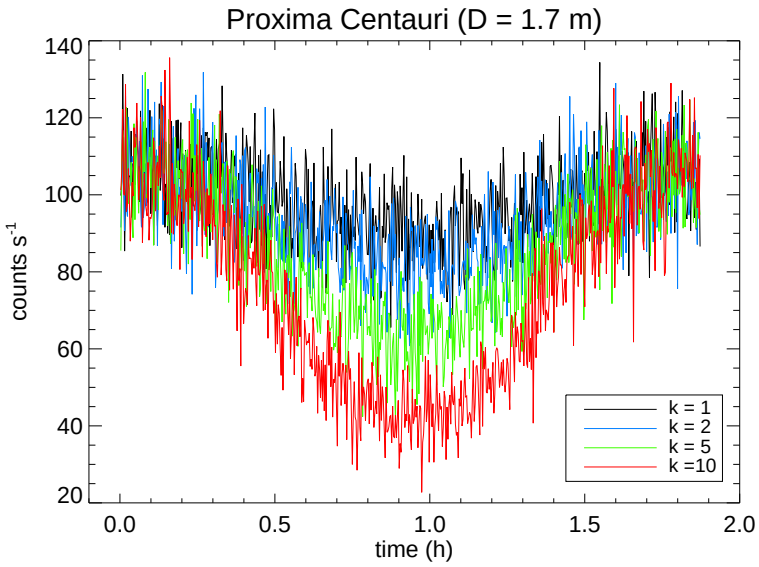

Fig. 4 Impact of the distribution of hydrogen in the exosphere in the transit light curve of Prox Cen as observed by WSO-UV. Models corresponding to κ = 1, 2, 5 and 10 are plotted for comparison.

However, WSO-UV is far too small to detect Earth-like planets orbiting in the habitable zone around stars bigger than an M3V type star, no to mention around G2V, solar like stars. In Figure 5, we have plotted the detectability

of transits as a function of the telescope size and the stellar Lyα luminosity for M type stars. For the plot, a Lyα transit is considered to be detectable if the depth of the transit in the light curve is above the 2σ detectability level after co-adding 10 transits observations (with the same configuration as in Section 3); this is a strong condition since a dedicated mission such as Kepler uses as many as 100 transits to increase the signal to noise ratio.

A quick search using the services of the Centre de Données Stellaires (Strasbourg, France) finds 80 stars within 5 pc around the Sun and 47 of them are single M-type star. Lyα fluxes have been measured for few of them (Youngblood et al. 2016). There are two M5V stars in the sample, GJ876 and GJ581, and their observed Lyα flux is 0.14×10^{-12} erg s^{-1} cm^{-2} and 0.04×10^{-12} erg s^{-1} cm^{-2}. According to Fig. 5, the exosphere of an Earth-like planet would be easily detectable with an 8 m primary space telescope by the transit method.

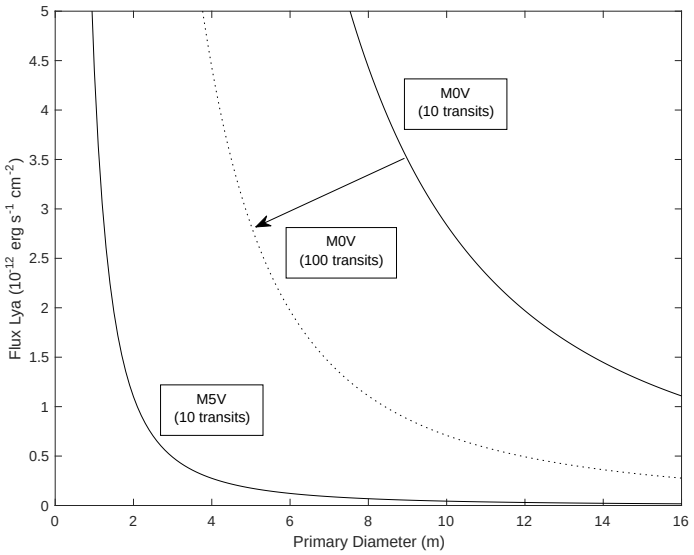

Fig. 5 Detectability of a transiting Earth analogue by flux variations in the Lyα line as a function of the observed Lyα flux (including interstellar absorption) and the diameter of the primary mirror of the telescope (see text for instrumentation configuration and detectability threshold definition).

5 Conclusions

To summarise, it is feasible to measure the distribution of exospheric hydrogen in terrestrial planets orbiting nearby cool M type stars with moderate size (4-8 m primary mirror) space observatories. These measurements are required to

understand the dominant processes in the upper atmospheric layers and the energy flow between the atmosphere and the surrounding space because very different levels of space weather can be tested. In this manner, the role of stellar activity and evolutionary state, i.e. the role of particle collisions and planetary magnetic fields in energising the neutral hydrogen atoms, could be addressed rigorously.

References

1. Anglada-Escudé, G., Amado, P.J., Barnes, J. 2016, Nature, 536, 437.
2. Berta-Thompson, Z.K., Irwin, J., Charbonneau, D. et al. 2016, Nature, 527, 204.
3. Benedict, G. F., Henry, T. J., Franz, O. G. et al. 2016, AJ, 152,5,141
4. Bourrier, V., Ehrenreich, D., King, G. et al. 2017, A&A, 597, 26.
5. Brasseur, G. and Solomon, S. 1996, Aeronomy of the middle atmosphere. Chemistry and Physics of the Stratosphere and Mesosphere. Atmospheric Science Library, 5, Springer Ed., ISBN: 978-90-277-2344-4.
6. Chamberlain, J.W. 1963, Planetary coronae and atmospheric evaporation. Planet. Space Sci., 11, 901 (1963).
7. Chen, C. H., Patten, B. M., Werner, M. W. et al. 2005, ApJ, 634, 1372
8. Dessler, A.E., Weinstock, E.M., Hintsa, E.J. et al. 1994, Geophysical Res. Letters, 21
9. Dressing, C. D. and Charbonneau, D. 2015, ApJ, 807, 45.
10. Ehrenreich, D., Bourrier, V., Bonfils, X., et al., 2012, A&A, 547, 18.
11. Ehrenreich, D., Bourrier, V., Wheatley, P. J. et al. 2015, Nature, 522, 459.
12. Fuselier, S. A., et al. 2000, Space Science Reviews, IMAGE special issue, 91, 51.
13. Gómez de Castro, A. I., Perea, G. B., , Sánchez, N. et al. 2014, ApSS, 354, 177.
14. Lallament, R., Clarke, J.T., Malam, Y., et al. 1996. Science with the Hubble Space Telescope-II, Space Telescope Institute, P. Benvenutti, F.D. Macchetto, E.J. Schreier, eds.
15. Lecavelier Des Etangs, A., Ehrenreich, D., Vidal-Madjar, A., et al. 2010, A&A, 514, 72.
16. Maldonado, J., Affer, L., Micela, G. et al. 2015, A&A, 577, 132.
17. McComas, D.J., Allegrini, F., Baldonado, J. et al. 2009, Space Science Reviews, 142, 157.
18. Mende, S. B., Heetderks, H., Frey, H. U. et al. 2000. Space Science Reviews, 91, 287.
19. Motalebi, F., Udry, S., Gillon, M., et al., 2015. A&A, 584, 72.
20. Oestgaard, N., Mende, S.B., Frey, H.U. et al. 2003. Journal of Geophysical Research, 108, NO. A7, 1300.
21. Pepe, F. et al. 2013. Nature, 503, 377-380.
22. Pourbaix, D., Boffin, H. M. H., 2016, A&A, 586, A90.
23. Qin, J., Waldrop, L. 2016. Nature Communications, 7, 13655.
24. Rairden, R. L., Frank, L. A. , Craven, J. D. 1986. J. Geophys. Res. 91, 3613.
25. Rhee, J.H., Song, I., Zuckerman, B. et al. 2007, ApJ, 660, 1556.
26. Shizgal, B. D. , Arkos, G. G. 1996. Rev. Geophys. 34, 483.
27. Vidal-Madjar, A., Lecavelier des Etangs, A., Désert, J.-M., et al. 2003, Nature, 422, 143.
28. Werner S., Keller, H.U. Korth, A. et al. 2004. Advances in Space Research, 34, 8, 1647.
29. Wood, B.E., Redfield, S., Linsky, J.L. et al. 2005. ApJSS, 159, 118.
30. Youngblood, A., France, K., Loyd, R.O.P. et al., 2016, ApJ, 824, 101
31. Zoennchen, J. H., Nass, U., Lay, G. & Fahr, H. J. 2010. Ann. Geophys. 28, 1221.